

***In situ* blistering observations on metals under proton irradiation**

A. Badtrudinov¹, T. Bykov^{2,3}, Y. Higashi¹, D. Kasatov^{2,3}, Ya. Kolesnikov^{2,3}, A. Koshkarev^{2,3}, A. Makarov^{2,3}, T. Miyazawa¹, I. Shchudlo^{2,3}, E. Sokolova^{2,3}, H. Sugawara¹, S. Taskaev^{2,3}

¹Advanced Medical Instrumentation Unit, Okinawa Institute of Science and Technology, 1919-1 Tancha, Onna-son, Kunigami-gun, Okinawa-ken, Japan 904-0495

²Budker Institute of Nuclear Physics, 11 Lavrentiev ave., 630090 Novosibirsk, Russia

³Novosibirsk State University, 2 Pirogov str., 630090 Novosibirsk, Russia

ABSTRACT

On a tandem accelerator with vacuum isolation, blistering of metal samples *in situ* was observed upon irradiation with 2 MeV protons to a fluence of $3.4 \pm 0.3 \cdot 10^{19} \text{ cm}^{-2}$. Copper and tantalum samples of different purities were placed in the path of the proton beam and forcibly cooled down. Sample surfaces were observed using a CCD camera with a remote microscope. Here we describe the experimental setup, results obtained, and their relevance to development of lithium targets of accelerator neutron sources for boron neutron capture therapy. To develop a promising technique for the treatment of malignant tumors, boron-neutron capture therapy [1, 2], an accelerator source of epithermal neutrons was proposed and created at the Budker Institute of Nuclear Physics [3, 4]. Neutron generation occurs as a result of the threshold reaction ${}^7\text{Li} (p, n) {}^7\text{Be}$ by directing a 2-MeV proton beam with a current of up to 5 mA, obtained in a vacuum-insulated tandem accelerator to a 10-cm diameter lithium target.

The target is made of a thin lithium layer sputtered onto a cooled copper substrate, in this case copper [5, 6]. The thickness of the lithium layer that generates neutrons is chosen in such a way that proton energy as they exit the layer is slightly below 1.882 MeV, the threshold of the ${}^7\text{Li} (p, n) {}^7\text{Be}$ reaction. Further deceleration and absorption of the protons occur in the structural material, upon which the following requirements are imposed. First, the material must have a high thermal conductivity or be thin enough that the temperature of lithium does not exceed its melting point of 182° C to prevent mixing of the radioactive isotope, ${}^7\text{Be}$, with the lithium vapor. To maintain high thermal conductivity, the best support material is copper. Secondly, deceleration of protons in this material should not lead to appreciable generation of unwanted X-rays and gamma rays. To avoid X-ray and gamma-radiation, the best materials are molybdenum and tantalum [7]. Third, this material must have sufficient resistance to radiation blistering [8, 9]. Deformation of the surface layer, evident in the formation of blisters and exfoliation of thin layers of material, decreases thermal conductivity. Experimental data on the magnitude of the critical dose for blister formation are extremely scarce, and there are no data for protons with energies in the region of 2 MeV. The blistering phenomenon is thought to be characteristic of metals that dissolve hydrogen poorly (Al, Mo, Fe, Cu, Ag, W, Pt, Au) [8, 9]. In metals in which hydrogen dissolves well (alkali, alkaline earth, Ti, Ta, Nb, V, Ni, Pd), blistering is not observed. The threshold for hydrogen blistering in copper, 10^{18} cm^{-2} [8, 9], limits the use of copper as a target substrate, since at a proton current of 10 mA and a target diameter of 10 cm the critical dose accumulates in 20 min, which is less than the planned time therapy (1 h). When irradiation was carried out with 200-keV protons and the copper temperature was ~100° C, the observed radiation dose causing the appearance of blisters in

copper was 10 times greater – 10^{19} cm^{-2} [10]. In copper irradiated with 2 MeV protons the estimated dose causing blisters to appear was $2 \times 10^{19} \text{ cm}^{-2}$ [2, p. 81]. We also obtained a similar value of $1.7 \times 10^{19} \text{ cm}^{-2}$ experimentally [2, p. 82]. Figure 1 is a photograph showing part of the surface of a copper substrate of a target purified from the lithium layer after generation of neutrons for biological studies [11]. The aim of the work was to study the formation of blisters during irradiation of copper and tantalum samples with protons having an energy of 2 MeV.

EXPERIMENTAL INSTALLATION

Investigations were carried out on a vacuum-insulated accelerator-tandem [3], which provides a 2-MeV proton beam, up to 5 mA, with a transverse dimension on the order of 1 cm [12]. The experimental setup is shown in Fig. 2. In the diagnostic tank of the proton beam transport path (6, in Figure 2), a sample disk 30 mm in diameter, and 3 mm thick was placed on the axis. The sample was pressed tightly against the heat sink surface using a liquid metal of gallium-indium alloy between the sample and the heat sink. The sample temperature ($\pm 1^\circ \text{C}$) was measured with a Pt100 platinum thermistor (CHEPT-1) inserted into a 1.5 mm hole drilled into the sample to the center of the disc at a depth of 1.5 mm below the surface. The thermistors were previously calibrated and connected in a three-wire circuit, taking into account the error introduced by the resistance of the wires. The surface temperature of the sample was measured using an Optris CT Laser 3ML SF pyrometer (Optris, GmbH, Germany). The current of the proton beam incident on the sample was measured with an ohmic divider when a positive voltage of 100 V was applied to the sample and a negative voltage of 300 V was applied to the suppressor ring, set 50 mm in front of the sample. A copper-cooled diaphragm with a hole 26 mm in diameter was installed in front of the diagnostic chamber. Temperature measurements with four Pt100 thermistors, inserted inside the diaphragm and uniformly spaced in azimuth, made it possible to control propagation of the proton beam along the axis of the apparatus. Continuous real-time monitoring of the sample surface was carried out through a fused quartz window using a CCD camera with an Infinity K2 remote microscope (DistaMax™, USA) (3 in Figure 2) installed at an angle of 42° to the sample surface normal (5 in Fig. 2). The distance from the surface of the front lens of the microscope to the sample was 330 mm. The microscope was calibrated with a 100- μm crosshair and a resolution of 260 lines / mm. Samples through an additional window of fused quartz were illuminated with a halogen lamp light source (LFP-10WP-R, Shibuya, Japan) with a power of 10 W (4 in Figure 2). Next to the CCD camera was a computer (2 in Figure 2) used to collect data from the camera, to save the images to a local database, and to display the status of the target in real time.

EXPERIMENTAL RESULTS

Four samples were examined. Three of them were made of different copper samples: copper, grade M0 (GOST 859-2014, Russia), fine-grained copper, 99.996% pure (OFC-1 JIS H3150 C1011, SH Copper Products Co., Ltd., Japan) and coarse-grained copper, 99.99996% (high-purity copper, Mitsubishi Materials Co., Japan). The fourth sample was made of tantalum, 99.7%. Copper samples were polished to a mirror surface of optical quality by means of diamond polishing. Samples were subjected to a 2-MeV proton beam, 0.6 mA current for 3 hours, at a temperature of $263^\circ \text{C} \pm 15^\circ$. The tantalum sample was irradiated with a proton beam at a current of 0.45 mA for 4 hours. Its temperature was 600°C . In all cases, the same current integral was sought, amounting to $1.81 \pm 0.03 \text{ mAh}$. The transverse dimension of the beam was determined in two ways. First, a proton beam-irradiated titanium sample without ensuring good thermal contact with the heat sink surface. After a short time, a hole 11 mm in diameter was bored into the sample (Fig. 3). Second, a proton beam-irradiated titanium sample with to ensuring good thermal contact with the heat sink surface. It also prevented burning holes

into and sputtering of the titanium. Since the interaction of protons with titanium leads to the operating time of radioactive isotopes of vanadium with half-lives of 33 min, 16 days, and 330 days, the area under the beam becomes radioactive. Its size was determined by measuring the activity of an sample with a NaI-gamma spectrometer by successively increasing the collimation opening from 8 to 20 mm in steps of 2 mm. By this method, the transverse beam dimension was determined as 12 ± 1 mm. Taking the diameter of the proton beam to be 12 ± 1 mm, we found that the samples were irradiated to a fluence of $3.4 \pm 0.3 \times 10^{19} \text{ cm}^{-2}$.

RESULTS

Under the proton beam, the M0 GOST 859-2014 grade copper and fine-grained copper samples behaved similarly. The first blisters began to appear at a fluence of about 10^{19} cm^{-2} . The entire sample surface was densely covered with blisters at fluence of $3.4 \times 10^{19} \text{ cm}^{-2}$. Figure 4 shows the dynamics of blister formation. The coarse-grained copper sample behaved quite differently. Figure 5 shows photographs of the sample surface at different irradiation fluences. Blisters in the form of bubbles on the surface were not formed, but the surface cracked due to the irradiation. Cracks began to appear at a fluence of $2 \times 10^{19} \text{ cm}^{-2}$. No evidence of blister formation was observed on the tantalum sample until the collected fluence was $3.4 \times 10^{19} \text{ cm}^{-2}$. Modifications of the sample surface from tantalum were not detected until the fluence reached $3.4 \times 10^{19} \text{ cm}^{-2}$.

CONCLUSION

Surfaces of metals were observed when irradiated with a 2-MeV proton beam, 1.2 cm in diameter to a fluence of $3.4 \pm 0.3 \times 10^{19} \text{ cm}^{-2}$. On the surfaces of M0 GOST and fine-grained copper samples heated to a temperature of $263 \pm 15^\circ \text{ C}$, with a proton fluence of 10^{19} cm^{-2} , blisters begin to appear, covering the surface densely at a fluence of $3 \times 10^{19} \text{ cm}^{-2}$. When heated to a temperature of $263 \pm 15^\circ \text{ C}$, the surface of the coarse-grained copper sample began to be covered with cracks at a proton fluence of $2 \times 10^{19} \text{ cm}^{-2}$. Modifications of the sample surface from tantalum at a temperature of 600° C were not detected until the fluence reached $3.4 \times 10^{19} \text{ cm}^{-2}$. The present results are important for development of a neutron-generating lithium target of an accelerating neutron source for boron-neutron capture therapy. With a target diameter of 10 cm, the time of appearance of blisters exceeds the planned length of neutron capture therapy; therefore, the target, made with a thin lithium layer sputtered onto a cooled copper substrate, can be used to generate neutrons for boron neutron capture therapy. The use of coarse-grained copper with a purity of 99.99996% can prolong the lifetime of the target, since radiation damage by the proton beam does not cause blistering that reduces the thermal conductivity. Instead, damage appears in the form of cracking, which has a lesser effect on thermal conductivity. Tantalum is more resistant to radiation blistering than copper.

ACKNOWLEDGMENTS

This study was carried out with a grant from the Russian Science Foundation (project No. 14-32-00006) with the support of the Budker Institute of Nuclear Physics and Novosibirsk State University. This is endorsed by the joint collaboration agreement between OIST and BINP Novosibirsk. Finally, we are grateful to the members of OIST Mechanical Engineering & Microfabrication Support Group for the technical support.

REFERENCES

1. W. Sauerwein, A. Wittig, R. Moss, Y. Nakagawa (Eds.), Neutron Capture Therapy. Principles and Applications, Springer, Heidelberg New York Dordrecht London, 2012.
2. S. Taskaev, V. Kanygin, Boron Neutron Capture Therapy, Publishing House of the SB RAS, Novosibirsk, 2016.
3. B. Bayanov, V. Belov, E. Bender, M. Bokhovko, G. Dimov, V. Kononov, O. Kononov, N. Kuksanov, V. Palchikov, V. Pivovarov, R. Salimov, G. Silvestrov, A. Skrinsky, and S. Taskaev, Nucl. Instr. Meth. A **413**, 397 (1998).
4. S. Taskaev, Physics of Particles and Nuclei **46**, 956 (2015).
5. B. Bayanov, V. Belov, V. Kindyuk, E. Oparin, S. Taskaev, Applied Radiation and Isotopes **61**, 817 (2004).
6. B. Bayanov, V. Belov, S. Taskaev, J. Phys.: Conf. Ser. **41**, 460 (2006).
7. D. Kasatov, A. Makarov, S. Taskaev, I. Shchudlo, Physics of Atomic Nuclei **78**, 905 (2015).
8. R. Behrisch (Ed.), Sputtering by Particle Bombardment II, Springer, New York, 1984.
9. M. Guseva, Yu. Martynenko, Soviet Phys. Uspekhi **24**, 996 (1981).
10. V. Astrelin, A. Burdakov, P. Bykov, I. Ivanov, A. Ivanov, Y. Jongen, S. Konstantinov, A. Kudryavtsev, K. Kuklin, K. Mekler, S. Polosatkin, V. Postupaev, A. Rovenskikh, S. Sinitskiy, E. Zubairov, J. Nucl. Mater. **396**, 43 (2010).
11. O. Volkova, L. Mechetina, A. Taranin, A. Zaboronok, K. Nakai, S. Lezhnin, S. Frolov, D. Kasatov, A. Makarov, I. Sorokin, T. Sycheva, I. Shchudlo, S. Taskaev, Russ. J. Radiology **97**, 283 (2016).
12. A. Ivanov, D. Kasatov, A. Koshkarev, A. Makarov, Yu. Ostreinov, I. Sorokin, S. Taskaev, I. Shchudlo, Techn. Phys. Letters **42**, 608 (2016).

FIGURE LEGENDS

Figure 1. Surface of the copper substrate of the target after irradiation with protons with an energy of 2 MeV at a fluence of $1.7 \times 10^{19} \text{ cm}^{-2}$, using a Jeol JCM-5700 electron microscope.

Figure 2. Photograph of the experimental setup: 1. Tandem accelerator with vacuum isolation; 2. Computer; 3. Remote microscope with CCD camera; 4. Backlight; 5 Fused quartz window; 6. Diagnostic vacuum chamber. The arrow schematically shows the direction of the 2-MeV proton beam.

Figure 3. Measurement of the hole in the titanium sample.

Figure 4. Dynamics of blister formation on the surface of fine-grained copper with a purity of 99.996% after bombardment with a 2-MeV proton beam.

Figure 5. Dynamics of blister formation on the surface of coarse-grained copper with a purity of 99.99996% after bombardment with a 2-MeV proton beam.

Figure 6. Dynamics of blister formation on the surface of Tantalum with a purity of 99.7% after bombardment with a 2-MeV proton beam.

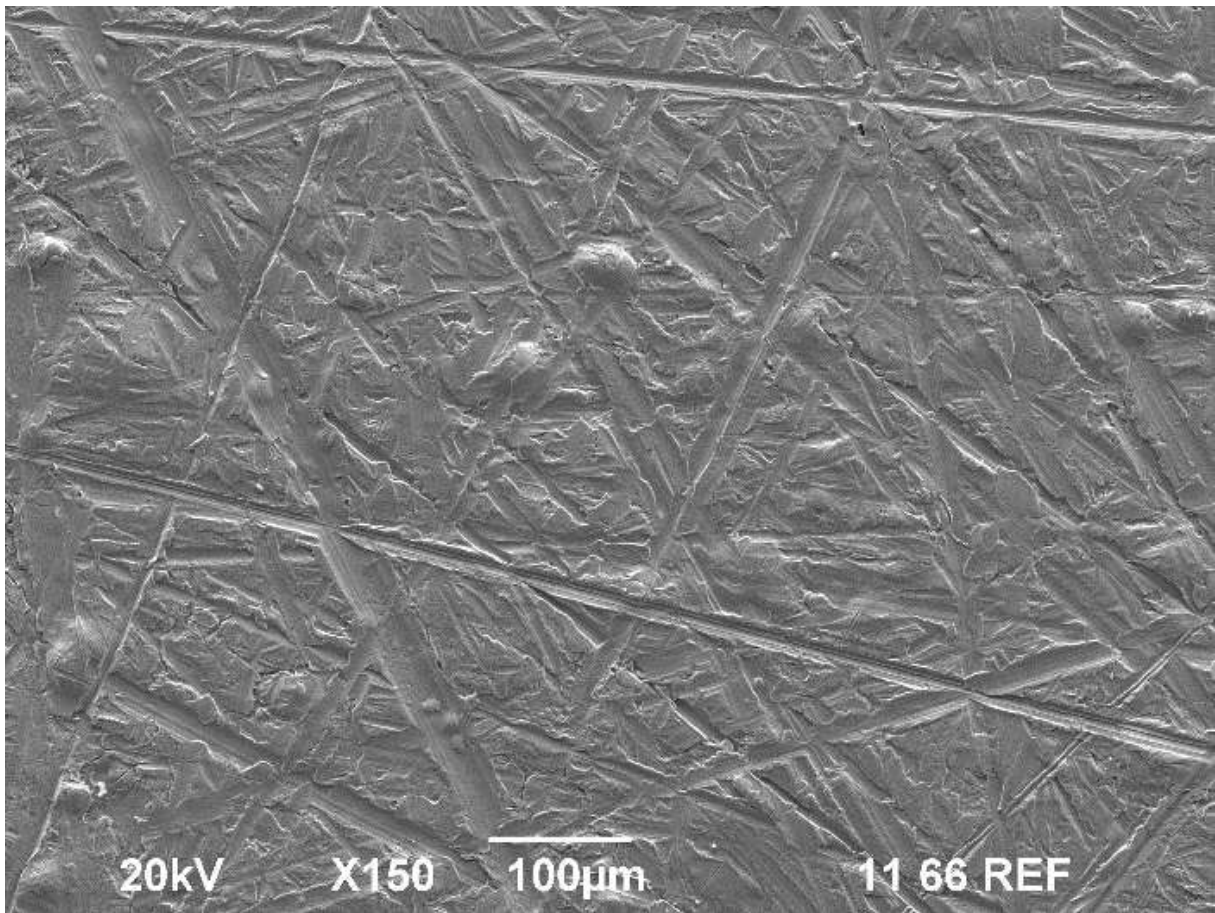


Figure 1.

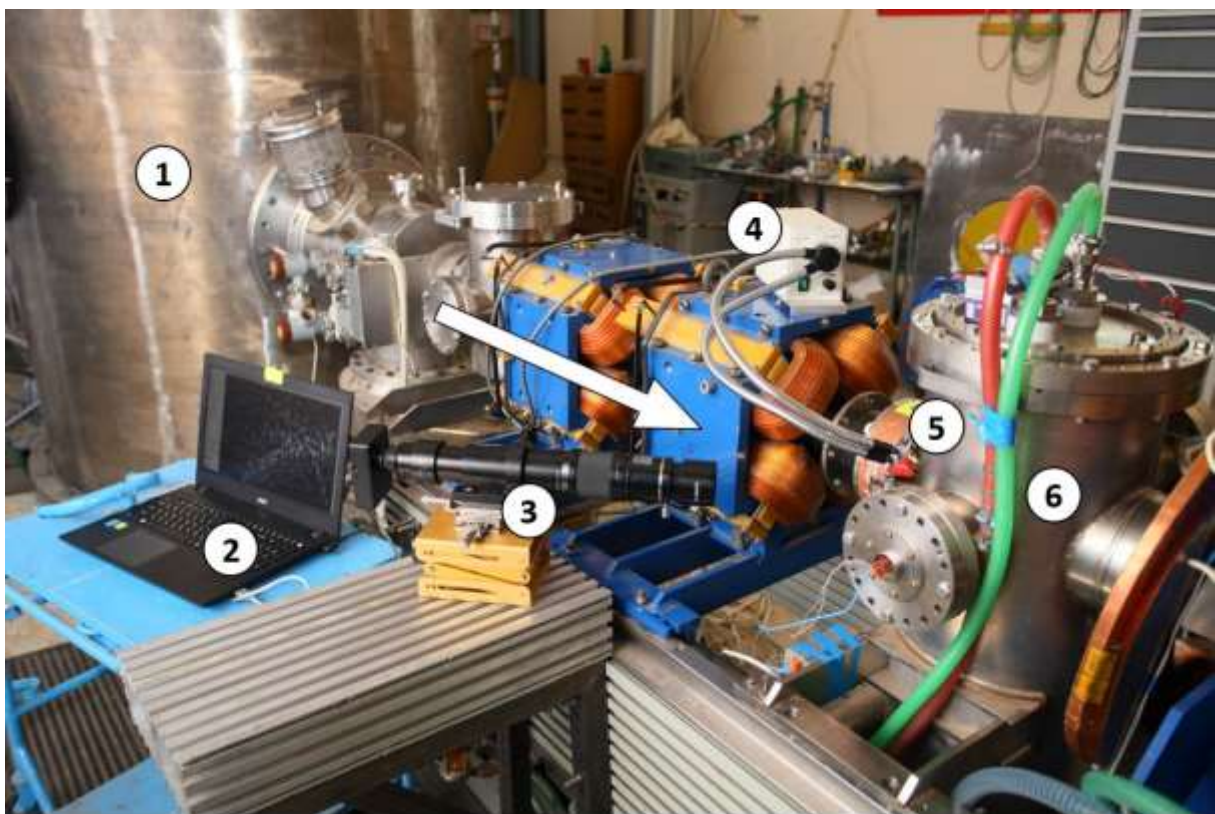


Figure 2.



Figure 3.

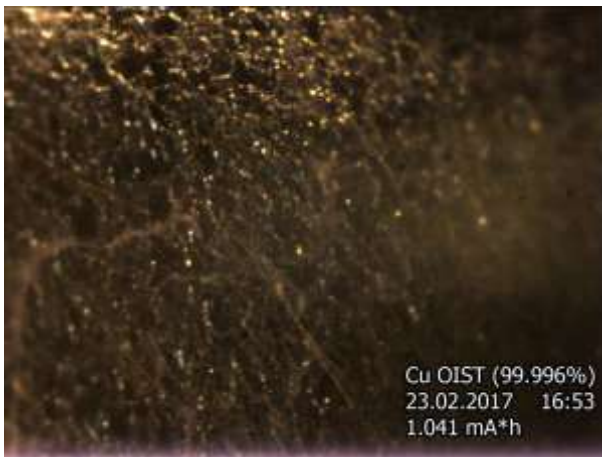
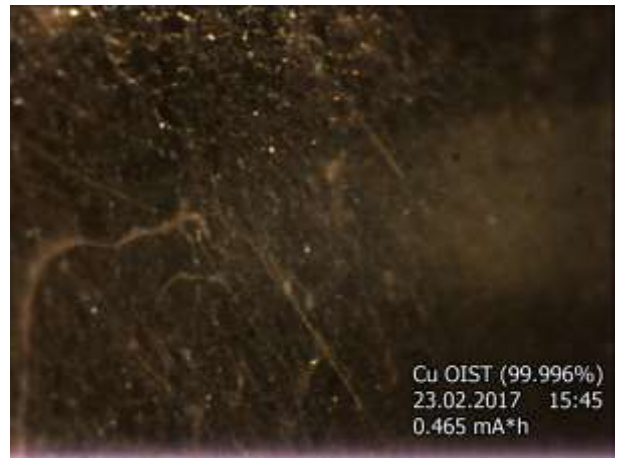
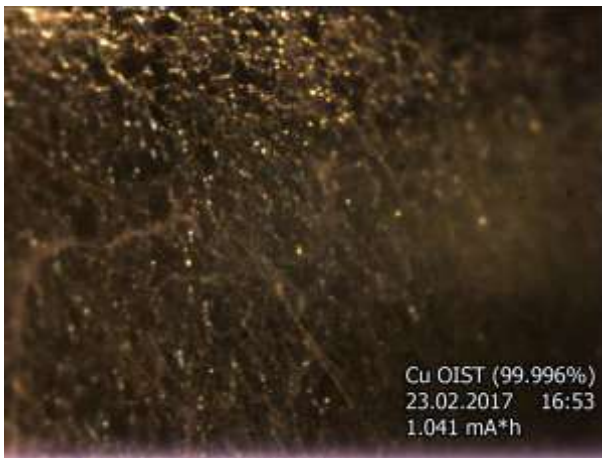


Figure 4.

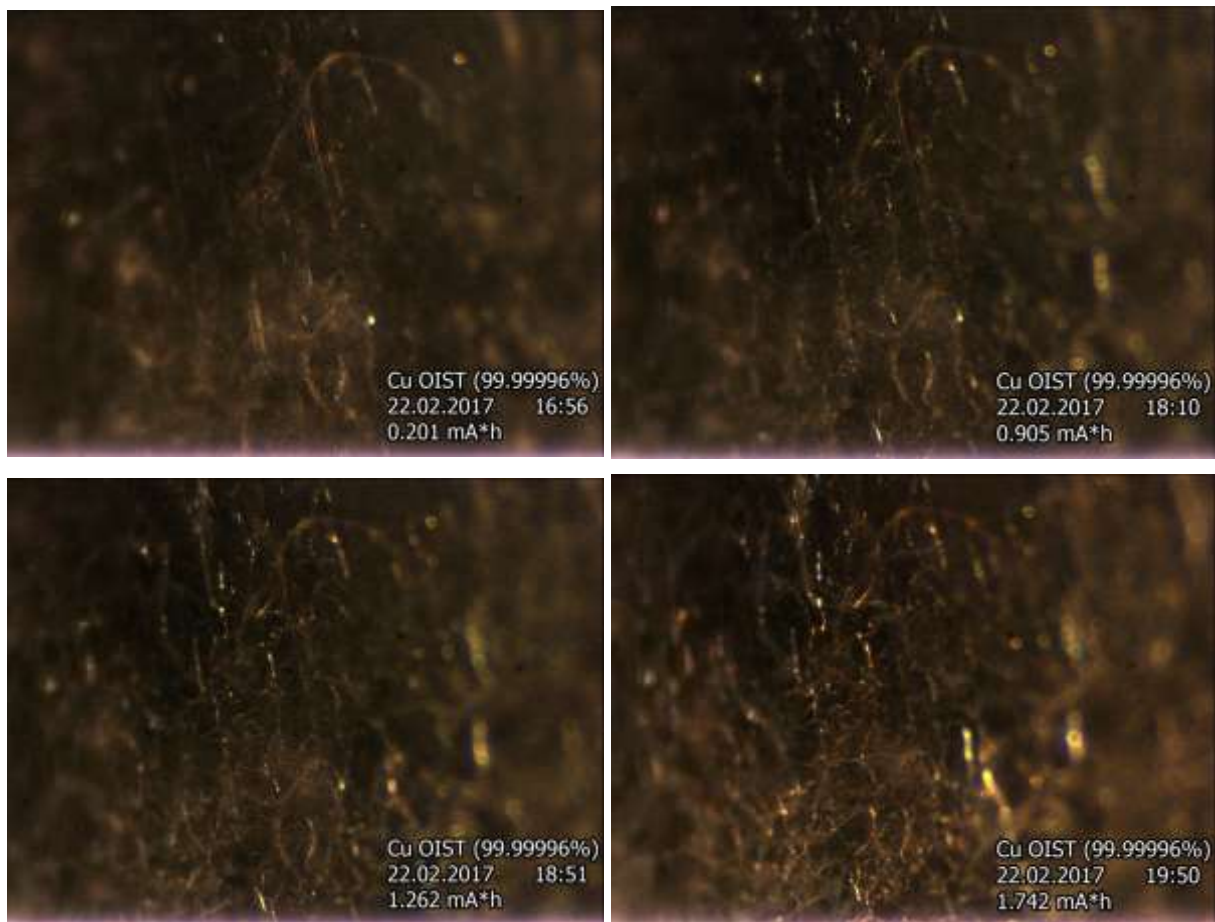


Figure 5.

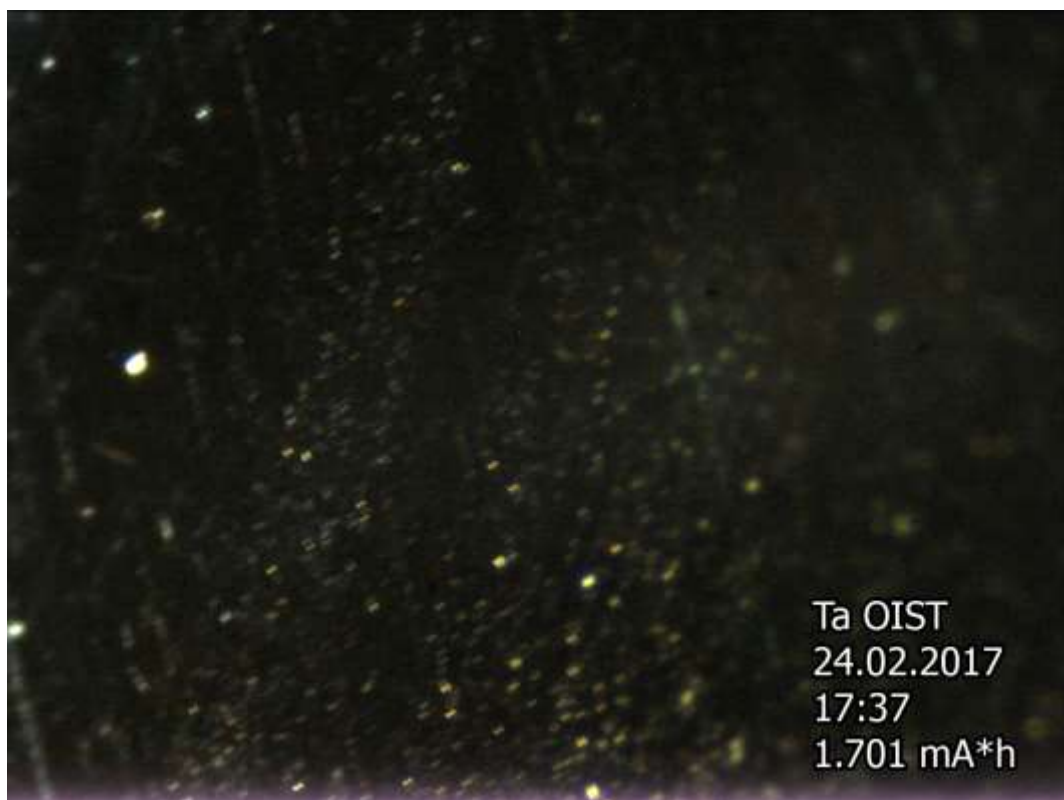


Figure 6.